# Low lattice thermal conductivity and high thermoelectric figure of merit in $Na_2MgSn$

Cong Wang,[1] Y. B. Chen,[2] Shu-Hua Yao,[1] and Jian Zhou[1,3,*]

[1]*National Laboratory of Solid State Microstructures and Department of Materials Science and Engineering, Nanjing University, Nanjing 210093, China*

[2]*National Laboratory of Solid State Microstructures and Department of Physics, Nanjing University, Nanjing 210093, China*

[3]*Collaborative Innovation Center of Advanced Microstructures, Nanjing University, Nanjing 210093, China*

(Received 17 July 2018; revised manuscript received 9 December 2018; published 23 January 2019)

Thermoelectric materials enables the harvest of waste heat and direct conversion into electricity. In search of high efficient thermoelectric materials, low thermal conductivity of a material is essential and critical. Here, we have theoretically investigated the lattice thermal conductivity and thermoelectric properties of layered intermetallic $Na_2MgSn$ and $Na_2MgPb$ based on the density functional theory and linearized Boltzmann equation with the single-mode relaxation-time approximation. It is found that both materials exhibit very low and anisotropic intrinsic lattice thermal conductivity. Despite the very low mass density and simple crystal structure of $Na_2MgSn$, its lattice thermal conductivities along $a$ and $c$ axes are only 1.77 and 0.81 W/m K respectively at room temperatures. When Sn is replaced by the heavier element Pb, its lattice thermal conductivities decrease remarkably to 0.56 and 0.31 W/m K respectively along $a$ and $c$ axes at room temperature. We show that the low lattice thermal conductivities of both materials are mainly due to their short phonon lifetimes and phonon mean free path. Combined with previous experimental measurements, the metallic $Na_2MgPb$ cannot be a good thermoelectric material. However, we predict that the semiconducting $Na_2MgSn$ is a potential room-temperature thermoelectric material with a considerable $ZT$ of 0.36 at 300 K. Our calculations not only imply that the intermetallic $Na_2MgSn$ is a potential thermoelectric material, but also can motivate more theoretical and experimental works on the thermoelectric researches in simple layered intermetallic compounds.

DOI: 10.1103/PhysRevB.99.024310

## I. INTRODUCTION

Thermoelectrical (TE) materials, which can directly convert heat to electricity, have been extensively studied for the last several decades since they play an important role in the area of environmentally friendly energy technology [1,2]. The conversion efficiency of TE materials is usually evaluated by a dimensionless figure of merit, $ZT = S^2\sigma T/\kappa$, where $S$, $\sigma$, $T$, and $\kappa$ are the Seebeck coefficient, electrical conductivity, absolute temperature, and thermal conductivity respectively. The thermal conductivity $\kappa$ of a material can be further divided into two items: $\kappa = \kappa_e + \kappa_L$, where $\kappa_e$ and $\kappa_L$ are electronic and lattice thermal conductivity respectively. For practical applications, the $ZT$ of a TE material should be at least larger than 1. A $ZT$ of 1 can have only 10% of Carnot efficiency. But a higher $ZT$ of 4 can realize 30% of Carnot efficiency and thus be comparable with many modern engines, such as home refrigeration [3]. However, these physical quantities ($S$, $\sigma$, and $\kappa$) in the same material are difficult to be tuned separately due to their internal relationship. In general, the electrical conductivity ($\sigma$) and electronic thermal conductivity ($\kappa_e$) will increase with the increase of carrier concentration, while the Seebeck coefficient ($S$) will decrease with it [1]. Therefore, most good TE materials are semiconductors, such as IV-VI compounds PbTe [4] and SnSe [5,6].

On the other hand, the lattice thermal conductivity ($\kappa_L$) is not directly related to the carrier concentration. Tuning the lattice thermal conductivities is an effective method to tune the $ZT$ values of materials. Typical materials with low lattice thermal conductivities are glasses. However, glasses are bad TE materials because of their very low carrier concentration and mobility compared with crystalline semiconductors [1]. Therefore, good TE materials require a rather peculiar property in the same system: "phonon-glass electron crystal" [7]. In other words, low lattice thermal conductivity is a necessary condition for good TE materials, although not a sufficient one.

In the classic physics picture, the lattice thermal conductivity can be approximated by the formula $\kappa_L = \frac{1}{3}C_v v l = \frac{1}{3}C_v v^2 \tau$, where $C_v$, $v$, $l$, and $\tau$ are the heat capacity, phonon velocity, mean free path (MFP), and relaxation time. Furthermore, the phonon velocity is often simply replaced by the sound velocity, which is proportional to $\sqrt{B/\rho}$, where $B$ and $\rho$ are the elastic modulus and mass density of a material [8]. Accordingly, one method to design low lattice thermal conductivity materials is to search for high density materials due to their low sound velocities, such as $Bi_2Te_3$. Besides, complex crystal structural materials usually have low sound velocities, such as $Yb_{14}MnSb_{11}$ [9]. The other way is to reduce the relaxation time by introduction of defects or nanostructures to scatter phonons [8]. Of course, the intrinsic large anharmonic effect (large Grüneisen parameters) in a material will also reduce the relaxation time by phonon-phonon scattering. A distinct example is SnSe, in which the large anharmonicity leads to its exceptional low lattice thermal conductivity [5]. However, it is not intuitive without quantitative calculations.

*Corresponding author: zhoujian@nju.edu.cn

 

In this work, we predict by first-principles calculations that the layered intermetallic $Na_2MgSn$ and $Na_2MgPb$ have very low and anisotropic intrinsic lattice thermal conductivities. Both materials have a very simple layered structure (eight atoms in the unit cell) and a low mass density (2.82 and 4.01 $g/cm^3$ for $Na_2MgSn$ and $Na_2MgPb$, respectively). In particular, we propose that $Na_2MgSn$ is a promising room-temperature TE material. An intermetallic is a solid-state compound exhibiting metallic bonding, defined stoichiometry, and ordered crystal structure. It is a large material family, which has a wide various crystal structure, ranging from 0 to 3 in dimensionality. Despite of their metallic bonding, some intermetallics are semiconductors, which is the precondition for their TE applications. There are many works about the potential TE intermetallic materials such as $Mg_3Sb_2$ [10–12], CaMgSi [13], $MGa_3$ ($M$ = Fe, Ru, and Os) [14], $YbAl_3$ [15], $Zn_4Sb_3$ [16], $Al_2Fe_3Si_3$ [17], $MIn_3$ ($M$ = Ru and Ir) [18], $M_2Ru$ ($M$ = Al and Ga) [19]. In particular, many half- and full-Heusler compounds, which are magnetic intermetallics, are found to be good TE materials [20–23].

In 2012, Yamada *et al.* reported the synthesis, crystal structure, and basic physical properties of hexagonal intermetallic $Na_2MgSn$ [24]. They found that polycrystalline $Na_2MgSn$ is a small band-gap semiconductor with a large Seebeck coefficient of $+390\ \mu V/K$ and an electrical resistivity of about 10 $m\Omega\,cm$ at 300 K. As a result, the power factor of $Na_2MgSn$ is almost 40% of that of $Bi_2Te_3$ [24]. Two years later, the same group synthesized the similar intermetallic $Na_2MgPb$ [25], which is a metal with three different phases from 300 to 700 K. In the experiment, the electrical resistivity of $Na_2MgPb$ is much lower than that of $Na_2MgSn$, which is only 0.4 $m\Omega\,cm$ at 300 K. From the preliminary experimental results, $Na_2MgSn$ could be a potential TE material. However, the thermal conductivity of $Na_2MgSn$ is not studied yet in both experiments [24,25] and the following theoretical work [26].

The rest of the paper is organized as follows. In Sec. II, we will give the computational details about phonon and thermal conductivity calculations. In Sec. III, we will present the main results about phonon dispersions, temperature, frequency dependent, and accumulated lattice thermal conductivity, group velocity, phonon lifetime, and Seebeck coefficient of $Na_2MgSn$ and $Na_2MgPb$. Some comparisons between different TE materials are also given. Finally, a short conclusion is presented.

## II. COMPUTATIONAL DETAILS

The structure of $Na_2MgSn$ and $Na_2MgPb$ are calculated by the Vienna ab initio simulation package (VASP) [27,28] based on the density functional theory. The projected augmented wave method [29,30] and the generalized gradient approximation with the Perdew-Burke-Ernzerhof exchange-correlation functional [31] are used. The plane-wave cutoff energy is set to be 350 eV. Both the internal atomic positions and the lattice constants are allowed to relax until the maximal residual Hellmann-Feynman forces on atoms are smaller than 0.001 eV/Å. An $8 \times 8 \times 4$ $k$ mesh was used in the optimization. We have tested that the van der Waals correction is not important in the two materials and thus not included in our calculations.

Both the second- and third-order interatomic force constants (IFCs) are calculated by the finite displacement method. The second-order IFCs in the harmonic approximation and the phonon dispersions of $Na_2MgSn$ and $Na_2MgPb$ are calculated by the PHONOPY code [32]. The third-order (anharmonic) IFCs and the lattice thermal conductivity are calculated by the PHONO3PY code [33]. We use a $2 \times 2 \times 2$ supercell (64 atoms) for the calculations of the second- and third-order IFCS in $Na_2MgSn$ and $Na_2MgPb$. And a $q$ mesh of $20 \times 20 \times 10$ is used for the calculation of lattice thermal conductivity by PHONO3PY code.

We do not use the crude force constants approximation in the third-order IFCs, although we have checked that a cutoff distance of 4 Å can already obtain a good thermal conductivity. We also checked a larger supercell of $3 \times 3 \times 2$ in $Na_2MgSn$ with a cutoff distance of 5 Å, and we found that the thermal conductivity changed little.

The Seebeck coefficients of $Na_2MgSn$ and $Na_2MgPb$ are calculated by the BOLTZTRAP2 program [34] with the Boltzmann transport theory. The electron eigenvalues in the whole Brillouin zone are calculated by the VASP code with the hybrid functional of Heyd-Scuseria-Ernzerhof (HSE06) [35] and spin-orbit coupling (SOC). A $k$ mesh of $20 \times 20 \times 10$ is used in the calculations of Seebeck coefficient.

## III. RESULTS AND DISCUSSIONS

### A. Crystal structure and phonon dispersions

As shown in Fig. 1(a), $Na_2MgSn$ and $Na_2MgPb$ share the same hexagonal crystal structure with the space group of $P6_3/mmc$ (no. 194). It is noted that $Na_2MgPb$ has three phases from 300 to 700 K [25]. However, from 300 to 500 K, $Na_2MgPb$ and $Na_2MgSn$ have the same hexagonal crystal structure [24,25]. Mg and Sn (or Pb) atoms lie in the same plane and form a two-dimensional (2D) honeycomb structure stacking along the $c$ axis. Two layers of Na atoms are intercalated between the adjacent Mg-Sn (or Mg-Pb) layers. This is a little different from other alkali-metal -intercalated layered materials, such as $Na_xCoO_2$ [36] or $Na_xRhO_2$ [37], in which only one Na layer is intercalated between the adjacent $CoO_2$ or $RhO_2$ layers. The Brillouin zone and high-symmetry $k$ points of $Na_2MgSn$ and $Na_2MgPb$ are given in Fig. 1(b).

The optimized lattice constants as well as the experimental ones of $Na_2MgSn$ and $Na_2MgPb$ are given in Table I. We

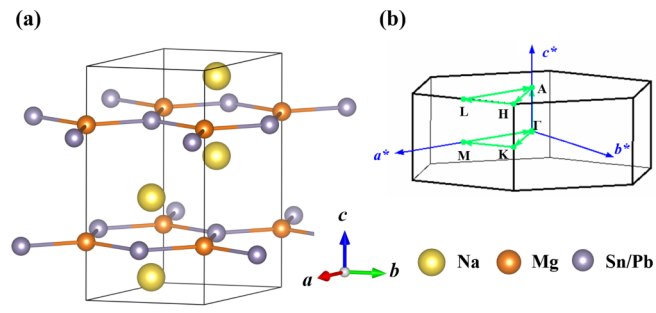


FIG. 1. (a) Layered crystal structure and (b) Brillouin zone and high-symmetry $k$ points of hexagonal $Na_2MgSn$ and $Na_2MgPb$.

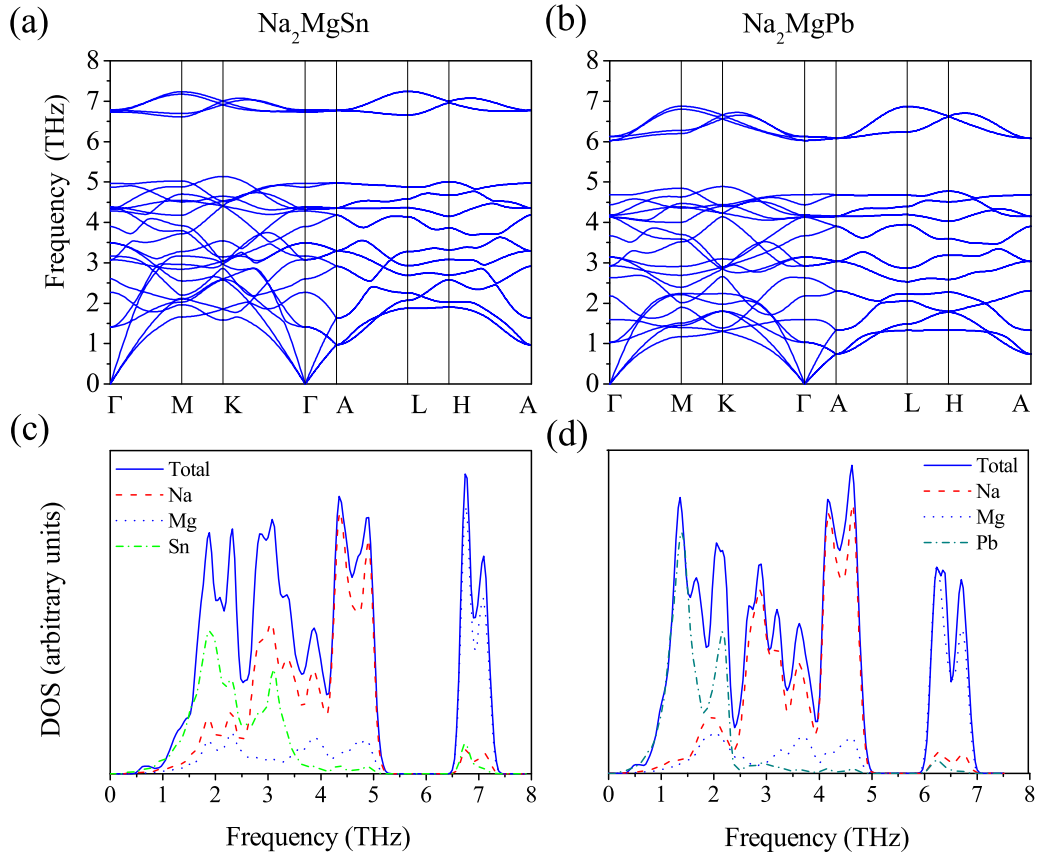


FIG. 2. Calculated phonon dispersions and density of states of hexagonal $Na_2MgSn$ (left column) and $Na_2MgPb$ (right column).

find that the theoretical and experimental lattice constants are very consistent with each other, with the largest difference less than 1%. Our calculated lattice constant is also consistent with Wang's calculation by the generalized gradient approximation with the ultrasoft pseudopotentials (GGA-USP). [26]

Based on the optimized structures, the phonon dispersions and density of states (DOS) of $Na_2MgSn$ and $Na_2MgPb$ are calculated by the PHONOPY code, given in Fig. 2. It is obvious that two materials show very similar phonon dispersions due to the same crystal structures. The highest frequency is about 7.5 and 7.0 THz for $Na_2MgSn$ and $Na_2MgPb$ respectively. There is also a clear band gap from 5 to 6.5 THz for $Na_2MgSn$ and from 5 to 6 THz for $Na_2MgPb$.

From the phonon DOS in Figs. 2(c) and 2(d), it is found that the high-frequency phonon modes above the band gap are mainly contributed from the vibrations of Mg ions. This feature is the same for $Na_2MgSn$ and $Na_2MgPb$. The main difference in phonon DOS between the two materials is the vibrations of Sn and Pb ions. Due to the larger atomic mass of Pb ions, the vibrational frequencies of Pb ions are mainly below 2.5 THz in $Na_2MgPb$, while the phonon modes of Sn ions extend from 0 to 4 THz in $Na_2MgSn$. The vibrations of Na ions are similar in both materials, which spread from 0 to 5 THz. It is also noted that the midfrequency phonon modes from 2.5 to 5 THz in $Na_2MgPb$ are mainly contributed from the vibrations of Na ions. However, for the phonon modes in the same frequency range in $Na_2MgSn$, there is also significant contribution from the vibrations of Sn ions. In other words, the vibrations of Na, Mg, and Pb ions in $Na_2MgPb$ are well separated in different frequency regions, while there is a relatively large overlap in $Na_2MgSn$.

TABLE I. Calculated and experimental lattice constants of hexagonal $Na_2MgSn$ and $Na_2MgPb$.

| Material | Method | $a$ (Å) | $c$ (Å) |
|---|---|---|---|
| $Na_2MgSn$ | present work | 5.0825 | 10.1075 |
| | expt. (293 K)[a] | 5.0486 | 10.0950 |
| | GGA-USP[b] | 5.0085 | 10.1314 |
| $Na_2MgPb$ | present work | 5.1415 | 10.1873 |
| | expt. (293 K)[c] | 5.1102 | 10.1714 |

[a]From Ref. [24].
[b]From Ref. [26].
[c]From Ref. [25].

### B. Lattice thermal conductivity

Based on the harmonic and anharmonic IFCs, we have calculated the lattice thermal conductivity ($\kappa_L$) by using the PHONO3PY code. Figure 3(a) shows the temperature-dependent thermal lattice conductivities along $a$ and $c$ axes of $Na_2MgSn$ and $Na_2MgPb$, while the average ones are also given in Fig. 3(b). It is quite surprising to find that the $\kappa_L$ of the two intermetallics are very low. As shown in Fig. 3 and Table II, the $\kappa_L$ of $Na_2MgSn$ is only 1.77 and 0.81 W/m K along $a$ and $c$ axes at 300 K, while it is even much lower for $Na_2MgPb$, which is 0.56 and 0.31 W/m K along $a$ and $c$

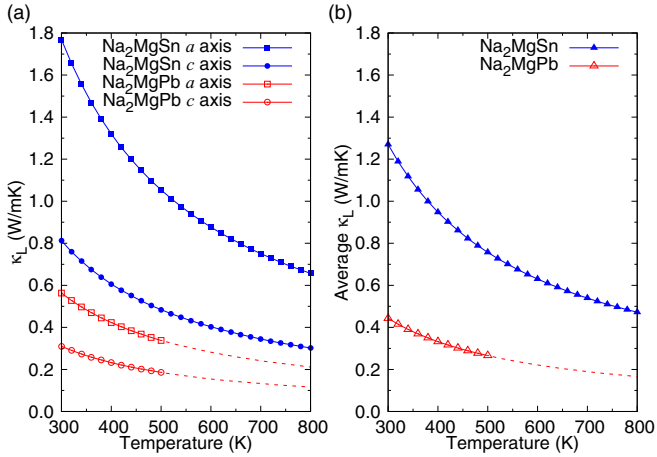


FIG. 3. (a) Calculated lattice thermal conductivities and (b) their average values of hexagonal $Na_2MgSn$ and $Na_2MgPb$ from 300 to 800 K. The red dashed lines mean that the high-temperature lattice thermal conductivities are calculated based on a low-temperature crystal structure of $Na_2MgPb$.

axes at the same temperature. Specifically, the $\kappa_L$ along the $c$ axis in $Na_2MgPb$ even approaches the predicted amorphous limit (0.25 W/m K) [38], which is extremely low for crystalline solids. The lattice thermal conductivity of $Na_2MgSn$ is comparable with the typical good TE materials, which will be discussed later. While the lattice thermal conductivity of $Na_2MgPb$ is even smaller than that of the recently found best TE material SnSe, which is 0.8, 2.0, and 1.7 W/m K along $a$, $b$, and $c$ axes at 300 K from the first-principles calculations [39]. It is noted that the lattice thermal conductivity of $Na_2MgPb$ above 500 K is meaningless since $Na_2MgPb$ has different crystal structures above that temperature. However, since we mainly focus on the room-temperature behavior of $Na_2MgPb$, it is not necessary to study its high-temperature thermal conductivity.

Furthermore, $Na_2MgSn$ and $Na_2MgPb$ both show an anisotropic lattice thermal conductivities due to their layered crystal structures. However, the ratio of thermal conductivities between the $a$ and $c$ directions in both materials is smaller than 2. The small anisotropy suggests that easily formed texture structures in layered compounds has not much effect on thermoelectric performance of these compounds.

We also calculated the average lattice thermal conductivity $\bar{\kappa}$, defined by the formula $3/\bar{\kappa} = 2/\kappa_a + 1/\kappa_c$, shown in Fig. 3(b) and Table II. The average $\bar{\kappa}$ for $Na_2MgSn$ and $Na_2MgPb$ are 1.27 and 0.44 W/m K at 300 K respectively.

The electronic thermal conductivity ($\kappa_e$) can be estimated by the Wiedemann-Franz law: $\kappa_e = LT\sigma$, where $L$ is the

TABLE II. Calculated lattice thermal conductivities $\kappa_a$ and $\kappa_c$ along $a$ and $c$ axes and their average value $\bar{\kappa}$ of hexagonal $Na_2MgSn$ and $Na_2MgPb$ at 300 K. The unit is W/m K.

| Material | $\kappa_a$ | $\kappa_c$ | $\bar{\kappa}$ |
|---|---|---|---|
| $Na_2MgSn$ | 1.77 | 0.81 | 1.27 |
| $Na_2MgPb$ | 0.56 | 0.31 | 0.44 |

TABLE III. Calculated sound velocities along $a$ and $c$ axes of $Na_2MgSn$ and $Na_2MgPb$. The unit is km/s.

| Material | $v_a$ | $v_c$ |
|---|---|---|
| $Na_2MgSn$ | 2.75 | 2.41 |
| $Na_2MgPb$ | 2.16 | 1.90 |

Lorenz number ($2.44 \times 10^{-8}$ W Ω K$^{-2}$), $\sigma$ is the electrical conductivity, and $T$ is the absolute temperature. Since the Wiedemann-Franz law is only applied to metals or heavily doped semiconductors and $Na_2MgSn$ is a semiconductor, we only use the Wiedemann-Franz law to calculate the electronic thermal conductivity of $Na_2MgPb$. According to previous experiments [25], we can obtain that the electrical resistivity ($\rho$) of $Na_2MgPb$ is about 0.4 mΩ cm at 300 K. So the electronic thermal conductivity of $Na_2MgPb$ is estimated to be 1.83 W/m K, which is even much larger than the lattice one. For the semiconducting $Na_2MgSn$, we just ignore its electronic thermal conductivity due to its semiconducting property.

The sound velocity is also calculated by the slopes of three acoustic-phonon branches near the Γ point (see Table III). For each direction, the sound velocity is averaged on the two transversal acoustic modes (TA1 and TA2) and one longitudinal acoustic mode (LA) by the formula $3/v_x^3 = 1/v_{x,\mathrm{TA1}}^3 + 1/v_{x,\mathrm{TA2}}^3 + 1/v_{x,\mathrm{LA}}^3$, where $x$ means the $a$ and $c$ axes. In Table III, we can see that in $a$ and $c$ axes, the sound velocities of $Na_2MgSn$ are both higher than those of $Na_2MgPb$. For both materials, the sound velocity along $a$ axis is higher than that along the $c$ axis.

We further plot the directional cumulative lattice thermal conductivity with respect to the phonon MFP in $Na_2MgSn$ and $Na_2MgPb$ at 300 K in Fig. 4. It is found that the $\kappa_L$ of $Na_2MgSn$ is mainly dominated by the phonons whose MFPs are less than 100 nm. However, for $Na_2MgPb$, the $\kappa_L$ is mostly contributed by the phonons whose MFPs are less than 20 nm. This indicates that the phonon MFP in $Na_2MgPb$ is much

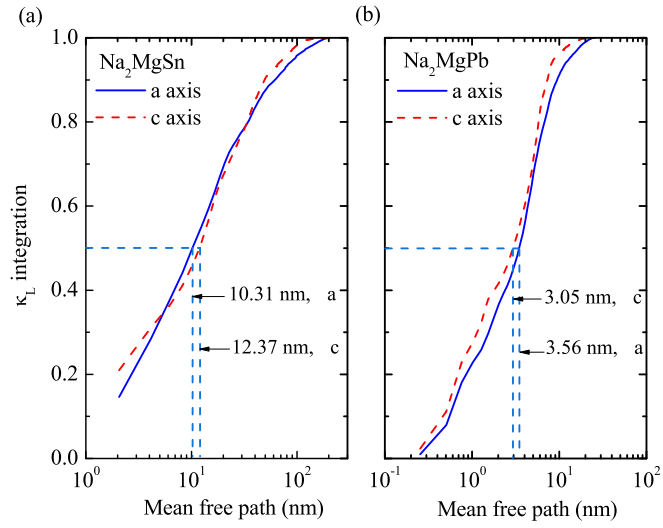


FIG. 4. Normalized directional accumulated lattice thermal conductivities of hexagonal (a) $Na_2MgSn$ and (b) $Na_2MgPb$ at 300 K.

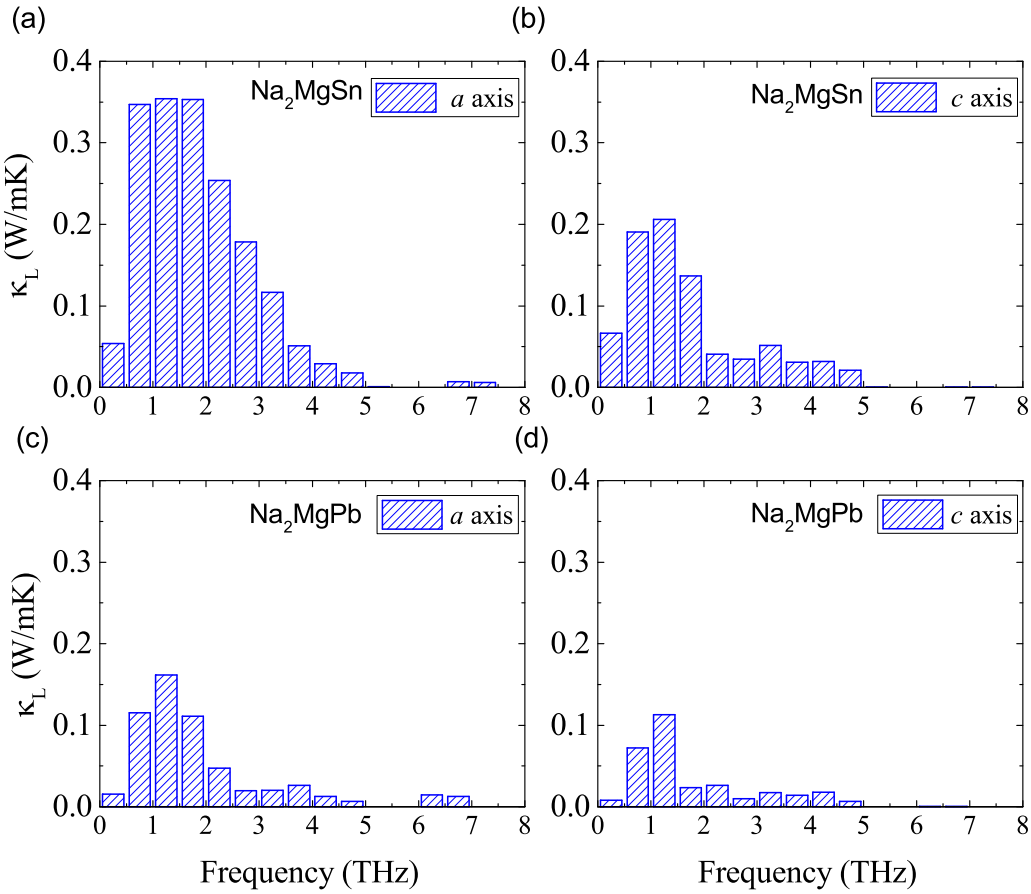


FIG. 5. Frequency-dependent lattice thermal conductivities of $Na_2MgSn$ and $Na_2MgPb$ at 300 K in $a$ and $c$ axes.

shorter than that in $Na_2MgSn$, leading to a much lower $\kappa_L$ in $Na_2MgPb$ than that in $Na_2MgSn$.

We also give the representative MFP (rMFP) for the two materials in Fig. 4. This parameter (rMFP) means that all the phonons whose MFP is shorter than the rMFP will contribute half to the total thermal conductivity. It is clear to see that the rMFP of $Na_2MgPb$ is much shorter than that of $Na_2MgSn$. For $Na_2MgSn$, the rMFP along the $a$ and $c$ axes are 10.31 and 12.37 nm respectively, while they are only 3.56 and 3.05 nm along the same axes for $Na_2MgPb$. The rMFP of $Na_2MgPb$ is even a little shorter than the ones of SnSe, which are 4.1, 4.9, and 5.6 nm along the $a$, $b$, and $c$ axes at 300 K from the first-principles calculations [39].

The length of the MFP in $Na_2MgSn$ is shorter than (or comparable with) the size of the crystalline grain of usual crystalline materials, therefore we think that the structural engineering, such as nanostructuring or polycrystalline structures, would be quite challenging in experiment to reduce the thermal conductivity in $Na_2MgSn$.

### C. Frequency-dependent lattice thermal conductivity

Here, we plotted the frequency-dependent lattice thermal conductivity of the two materials, as shown in Fig. 5. In this figure, the width of each column in the histogram is 0.5 THz. The summation of all columns is the total lattice thermal conductivity. In Figs. 5(a) and 5(b), the acoustic and low-frequency optical phonons below 3 THz contribute most of the thermal conductivity in $Na_2MgSn$ (about 87% along $a$ axis and 83% along $c$ axis). Similarly, in Figs. 5(c) and 5(d), the phonons below 3 THz contribute about 84% of the thermal conductivity along the $a$ axis and 82% along the $c$ axis in $Na_2MgPb$. On the other hand, the high-frequency optical phonons above the energy gap have negligible contribution to the thermal conductivity.

We also can directly compare the lattice thermal conductivity between $Na_2MgSn$ and $Na_2MgPb$, since we give the absolute value in Fig. 5. For example, in Figs. 5(a) and 5(c), we can find that the frequency-dependent lattice thermal conductivities of $Na_2MgPb$ along the $a$ axis are much smaller than those of $Na_2MgSn$ in the most of the frequency region (from 0 to 6 THz). Similar behavior can be found in the thermal conductivity along the $c$ axis.

### D. Group velocity and phonon lifetime

In order to further understand the low intrinsic thermal lattice conductivity in $Na_2MgSn$ and $Na_2MgPb$, we also calculated their frequency-dependent phonon group velocities and phonon lifetimes. In Fig. 6, we have given the squares of phonon group velocities of $Na_2MgSn$ and $Na_2MgPb$, since the lattice thermal conductivity is proportional to the squares of the phonon group velocities. We can see that the squares of the group velocities of $Na_2MgPb$ are smaller than those of $Na_2MgSn$, which results in the lower thermal conductivity in $Na_2MgPb$.

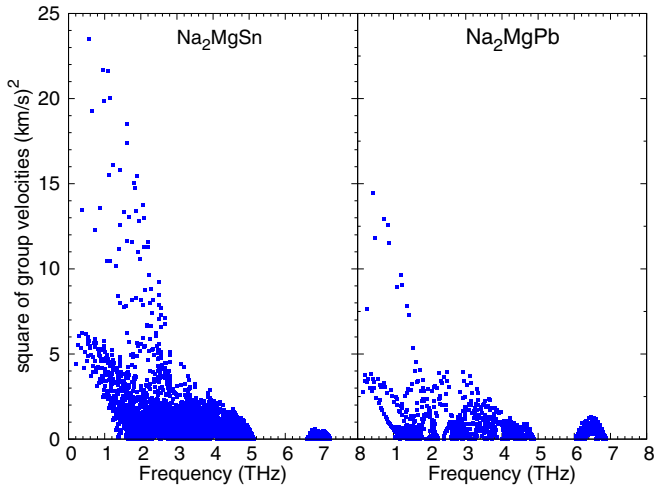


FIG. 6. Calculated square of the group velocities of $Na_2MgSn$ (left) and $Na_2MgPb$ (right).

The frequency-dependent phonon lifetimes of $Na_2MgSn$ and $Na_2MgPb$ are also calculated by the PHONO3PY code from third-order anharmonic IFCs, plotted in Fig. 7. The color bar in Fig. 7 represent the density of phonon modes. In general, we found that the phonon lifetimes of both materials are very short, roughly ranging from 0.4 to 4.5 ps, which are even smaller than those of SnSe (from 0 to 30 ps) [39]. Overall, the lifetimes of the low-frequency phonons below the band gap in $Na_2MgSn$ and $Na_2MgPb$ are similar, both showing a broad distribution with a maximal value about 4.5 ps. But relatively, $Na_2MgPb$ has more phonon modes with shorter lifetimes than those of $Na_2MgSn$ (particularly near 3 THz), which partially accounts for the lower thermal conductivity of $Na_2MgPb$. On the other hand, the lifetimes of high-frequency phonons above the band gap in the two materials are almost the same; both have a narrow distribution from 0.5 to 1.0 ps.

From the results of frequency-dependent lattice thermal conductivities, group velocities, and phonon lifetimes (from Figs. 5–7), we can conclude that lower group velocities and shorter lifetimes both contribute to the lower thermal conductivity of $Na_2MgPb$ compared with the one of $Na_2MgSn$.

### E. Seebeck coefficient

In order to estimate the $ZT$, we have also calculated the Seebeck coefficient of two materials, shown in Fig. 8. The electron band structure calculations with HSE06 hybrid functionals and SOC indicate that $Na_2MgSn$ is a small gap (about 0.18 eV) semiconductor, while $Na_2MgPb$ is a semimetal. In Fig. 8(a), the maximal absolute Seebeck coefficient of $Na_2MgSn$ at 300 K is about 250 $\mu$V/K, which is lower than the experimental value (390 $\mu$V/K). The difference of the theoretical and experimental Seebeck coefficient is due to the inaccurate theoretical band gap. In fact, we have also calculated the Seebeck coefficient of $Na_2MgSn$ with hybrid functionals but without SOC and the maximal Seebeck coefficient can reach 480 $\mu$V/K at 300 K (with a band gap of 0.34 eV). In Fig. 8(b), it is natural to find that the Seebeck coefficient of metallic $Na_2MgPb$ is quite low. At the Fermi energy, its Seebeck coefficient is about $-22$ $\mu$V/K.

### F. Discussion

First, we compare some theoretical physical properties of $Na_2MgSn$ and $Na_2MgPb$ with other well-known TE materials, such as SnSe, SnS, $Bi_2Te_3$, and PbTe, shown in Table IV. It is found that $Na_2MgSn$ and $Na_2MgPb$ have comparable lattice thermal conductivities as those TE materials. The main difference is that $Na_2MgSn$ and $Na_2MgPb$ have a much smaller mass density, a smaller bulk modulus, and a relatively higher sound velocity. In particular, the mass density of $Na_2MgSn$ is less than half of the SnSe's, while they almost have the same lattice thermal conductivities. It is a quite unique behavior in low-$\kappa$ materials. In spite of the very low mass density and

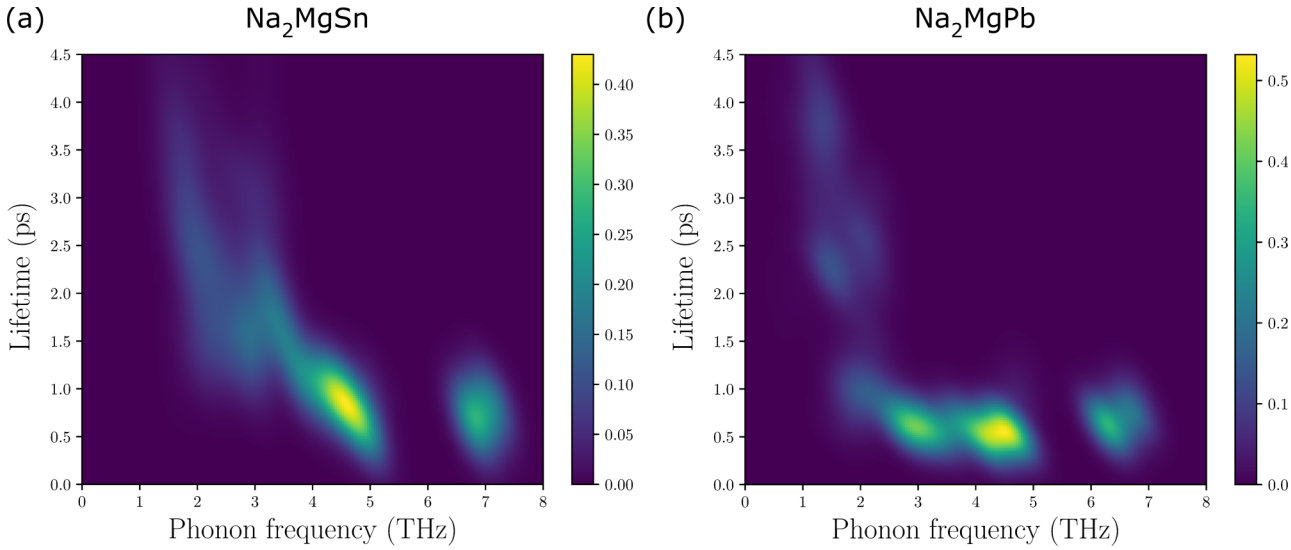


FIG. 7. Calculated phonon lifetimes of (a) $Na_2MgSn$ and (b) $Na_2MgPb$ at 300 K. The color in the figure represents the phonon density. Brighter color means a higher phonon density.

TABLE IV. Comparison of theoretical lattice thermal conductivity ($\kappa_L$), mass density ($\rho$), bulk modulus ($B$), sound velocity ($v$), rMFP, and maximal phonon lifetime ($\tau$) of $Na_2MgSn$ and $Na_2MgPb$ at 300 K with other typical TE materials. All physical quantities except the mass density are theoretical ones. The data of $Na_2MgSn$ and $Na_2MgPb$ are from the present work. The (a), (b), and (c) in the table indicates the $a$, $b$, and $c$ axes respectively.

| Material | $\kappa_L$ (W/m K) | $\rho$ (g/cm$^3$) | $B$ (GPa) | $v$ (km/s) | rMFP (nm) | $\tau$ (ps) |
|---|---|---|---|---|---|---|
| $Na_2MgSn$ | 1.77(a)/0.81(c) | 2.82 [24] | 30.6 | 2.75(a)/2.41(c) | 10.31(a)/12.37(c) | ~4.5 |
| $Na_2MgPb$ | 0.56(a)/0.31(c) | 4.01 [25] | 27.0 | 2.16(a)/1.90(c) | 3.56(a)/3.05(c) | ~4.5 |
| SnSe [39] | 0.8(a)/2.0(b)/1.7(c) | ~6.1 [42] | 39.4 | 0.40(a)/0.63(b)/0.58(c) | 5.6(a)/4.9(b)/4.1(c) | ~30 |
| SnS [39] | 0.9(a)/2.3(b)/1.6(c) | 5.1 [43] | 41.6 | 0.44(a)/0.71(b)/0.60(c) | 4.3(a)/5.2(b)/4.0(c) | ~30 |
| $Bi_2Te_3$ | 1.2(a)/0.4(c) [44] | 7.88 [45] | 36.4 [45] | 1.68(a)/1.79(c) [46] | 1.5(a) [44] | |
| PbTe | 2.1 [47] | 8.24 [48] | 45.51 [49] | 1.98 [49] | 6 [47] | ~100 [47] |

high sound velocity, $Na_2MgSn$ and $Na_2MgPb$ show a very low lattice thermal conductivity due to their large anharmonicity. From Table IV, we can see that the maximal lifetime of $Na_2MgSn$ and $Na_2MgPb$ is much smaller than those of SnSe, SnS, $Bi_2Se_3$, and PbTe. We think the large anharmonicity is probably due to the Na intercalated layered structures. In $Na_2MgSn$ and $Na_2MgPb$, there are two layers of Na ions loosely confined between adjacent Mg-Sn (or Mg-Pb) layers. The possible rattling modes of the Na ions could suppress the lattice thermal conductivity, as has been found in some cage structure materials, such as $Ba_8Ga_{16}Ge_{30}$ [40] and layered structure materials, such as $Na_xCoO_2$ [41].

Second, we can compare some experimental properties of $Na_2MgSn$ and $Na_2MgPb$ with other TE materials, as shown in Table V. It is found that $Na_2MgSn$ has a high Seebeck coefficient at room temperatures, which is much higher than those of $Bi_2Te_3$ and PbTe, but a little lower than those of SnSe and SnS. The calculated thermal conductivity of $Na_2MgSn$ is larger than that of SnSe, but lower than that of $Bi_2Te_3$ and PbTe. The main drawback of $Na_2MgSn$ is its low electrical conductivity, which is almost one order lower than that of $Bi_2Te_3$. Based on the experimental and calculated data in Table V, we can estimate that the $ZT$ of $Na_2MgSn$ is about 0.36 at 300 K, which is lower than that of $Bi_2Te_3$, but much higher than those of PbTe, SnSe, and SnS at the same temperatures. It is noted that the SnSe and SnS have the best performance at high temperatures (more than 700 K), while $Na_2MgSn$ would have the highest $ZT$ near the room temperature due to its small band gap.

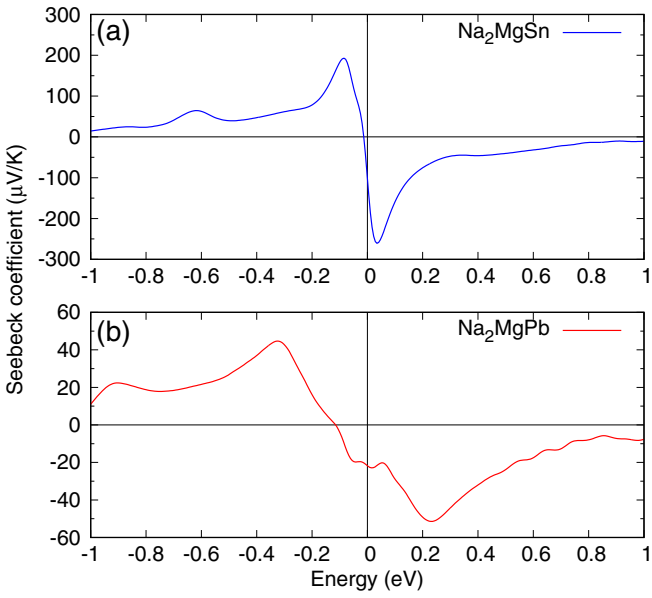


FIG. 8. Calculated Seebeck coefficient of (a) $Na_2MgSn$ and (b) $Na_2MgPb$ at 300 K. The Fermi energy is set to 0.

On the other hand, although $Na_2MgPb$ has an ultralow lattice thermal conductivity, its total thermal conductivity (about 2.27 W/m K) is not small due to the extra contribution of electrons. Its Seebeck coefficient is also very small (about 22 $\mu$V/K) due to its metallicity. Therefore the metallic $Na_2MgPb$ cannot be a good TE material, with an estimated $ZT$ of 0.016 at 300 K.

Finally, we would like to give some possible suggestions on how to improve the $ZT$ of $Na_2MgSn$. From Table V, the estimated $ZT$ of $Na_2MgSn$ is much lower than that of typical TE material $Bi_2Te_3$ at 300 K, because its electrical conductivity is ten times lower than that of $Bi_2Te_3$. Therefore, it is natural to think that if we can improve the electrical conductivity of $Na_2MgSn$, then we can possibly improve its $ZT$. The experimental electrical conductivity is measured based on the polycrystalline sample. If we can grow single crystalline $Na_2MgSn$, its electrical conductivity could be improved significantly. We note that the thermal conductivity of $Na_2MgSn$ used here is theoretical value, which is of course based on a perfect single crystal. Furthermore, we assume that the Seebeck coefficient will not change significantly from polycrystal to single crystal. If the electrical conductivity of single crystalline $Na_2MgSn$ could increase three times compared with the one of polycrystal, then its $ZT$ could possibly be larger than 1.

On the other hand, $Na_2MgPb$ has a much higher electrical conductivity than those of $Na_2MgSn$ and $Bi_2Te_3$, then the Pb doping in $Na_2MgSn$ could improve the electrical conductivity, thus the $ZT$ value.

It is also possible to improve $ZT$ by reducing the thermal conductivity of $Na_2MgSn$. According to the accumulated lattice thermal conductivities in Fig. 4(a), if we want to reduce 50% of the thermal conductivity of $Na_2MgSn$, we need to reduce the maximal MFP to about 10 nm by using the structural engineering methods, such as tuning the grain size of polycrystalline sample or making nanostructures. However, this could be quite challenging in experiment due to the very

TABLE V. Comparison of experimental electrical conductivity ($\sigma$), absolute Seebeck coefficient ($S$), total thermal conductivity ($\kappa$), and figure of merit $ZT$ of $Na_2MgSn$ and $Na_2MgPb$ at 300 K with other TE materials. The values with $*$ are theoretical ones or estimated ones based on the theoretical results. In the table, only SnSe sample is a single crystal.

| Material | $\sigma$ ($\Omega^{-1}$ cm$^{-1}$) | $S$ ($\mu$V/K) | $\kappa$ (W/m K) | $ZT$ |
|---|---|---|---|---|
| $Na_2MgSn$ [24] | 100 | 390 | 1.27* | 0.36* |
| $Na_2MgPb$ [25] | 2500 | 22* | 2.27* | 0.016* |
| SnSe [5] | 1.6(a)/10(b)/10.3(c) | 542(a)/522(b)/515(c) | 0.46(a)/0.7(b)/0.68(c) | 0.03(a)/0.12(b)/0.12(c) |
| SnS [50] | 0.001 | 400 | 1.25 | $3.8 \times 10^{-6}$ |
| $Bi_2Te_3$ [51] | 962 | 226 | 1.47 | 1.003 |
| PbTe [48] | 200 | 192 | 1.7 | 0.13 |

short phonon MFP. On the other hand, the atomic doping in $Na_2MgSn$ by Pb or other ions could also reduce the thermal conductivity by introducing more.

## IV. CONCLUSIONS

We have studied the lattice thermal conductivities and thermoelectric properties of layered intermetallic $Na_2MgSn$ and $Na_2MgPb$ based on the density functional theory and linearized Boltzmann equation. Despite their very low mass density and simple crystal structure, both materials exhibit very low lattice thermal conductivities, compared with other well-known TE materials. The lattice thermal conductivities along $a$ and $c$ axes of $Na_2MgSn$ are 1.77 and 0.81 W/m K respectively at 300 K, and they are much lower in $Na_2MgPb$, which are 0.56 and 0.31 W/m K along $a$ and $c$ axes at the same temperature. The main reason of their low thermal conductivity is due to their short phonon lifetimes and phonon mean free path.

$Na_2MgPb$ cannot be a good TE material due to its metallicity. However, we predict that $Na_2MgSn$ is a potential room-temperature TE material with a considerably large $ZT$ of 0.36. We also suggest that the $ZT$ of $Na_2MgSn$ could be further improved by a different method, such as growing single crystalline $Na_2MgSn$, doping Pb or other ions in $Na_2MgSn$, tuning the grain size of polycrystalline sample, or making nanostructures in $Na_2MgSn$.

Since the intermetallic is a large material family, our work can possibly stimulate further experimental and theoretical works about the thermoelectric research in simple layered intermetallic compounds.

*Note Added.* Recently, B. Peng *et al.* predicted that $Na_2MgPb$ is a Dirac semimetal, while $Na_2MgSn$ is a trivial indirect semiconductor with a small band gap of about 0.13 eV (with SOC) or 0.29 eV (without SOC) [52].

## ACKNOWLEDGMENTS

We thank Dr. Y. Han for invaluable discussions. This work was supported by the National Key R&D Program of China (Grant No. 2016YFA0201104) and the National Natural Science Foundation of China (Grants No. 11890702 and No. 51721001). The use of computational resources in the High Performance Computing Center of Nanjing University for this work is also acknowledged.

[1] G. J. Snyder and E. S. Toberer, Nat. Mater. **7**, 105 (2008).
[2] M. Zebarjadi, K. Esfarjani, M. S. Dresselhaus, Z. F. Ren, and G. Chen, Energy Environ. Sci. **5**, 5147 (2012).
[3] F. J. DjSalvo, Science **285**, 703 (1999).
[4] J. P. Heremans, V. Jovovic, E. S. Toberer, A. Saramat, K. Kurosaki, A. Charoenphakdee, S. Yamanaka, and G. J. Snyder, Science **321**, 554 (2008).
[5] L. D. Zhao, S. H. Lo, Y. Zhang, H. Sun, G. Tan, C. Uher, C. Wolverton, V. P. Dravid, and M. G. Kanatzidis, Nature (London) **508**, 373 (2014).
[6] C. Chang, M. Wu, D. He, Y. Pei, C. F. Wu, X. Wu, H. Yu, F. Zhu, K. Wang, Y. Chen, L. Huang, J. F. Li, J. He, and L. D. Zhao, Science **360**, 778 (2018).
[7] G. A. Slack, in *CRC Handbook of Thermoelectrics*, edited by D. M. Rowe (CRC Press, Boca Raton, 1995), pp. 407–440.
[8] E. S. Toberer, A. Zevalkink, and G. J. Snyder, J. Mater. Chem. **21**, 15843 (2011).
[9] S. R. Brown, S. M. Kauzlarich, F. Gascoin, and G. J. Snyder, Chem. Mater. **18**, 1873 (2006).
[10] W. Peng, G. Petretto, G. M. Rignanese, G. Hautier, and A. Zevalkink, Joule **2**, 1879 (2018).
[11] C. L. Condron, S. M. Kauzlarich, F. Gascoin, and G. J. Snyder, J. Solid State Chem. **179**, 2252 (2006).
[12] A. Bhardwaj, A. Rajput, A. K. Shukla, J. J. Pulikkotil, A. K. Srivastava, A. Dhar, G. Gupta, S. Auluck, D. K. Misra, and R. C. Budhani, RSC Adv. **3**, 8504 (2013).
[13] N. Miyazaki, N. Adachi, Y. Todaka, H. Miyazaki, and Y. Nishino, J. Alloys Compd. **691**, 914 (2017).
[14] Y. Amagai, A. Yamamoto, T. Lida, and Y. Takanashi, J. Appl. Phys. **96**, 5644 (2004).
[15] J. Liang, D. Fan, P. Jiang, H. Liu, and W. Zhao, Intermetallics **87**, 27 (2017).
[16] R. Carlini, D. Marre, I. Pallecchi, R. Ricciardi, and G. Zanicchi, Intermetallics **45**, 60 (2014).
[17] Y. Takagiwa, Y. Isoda, M. Goto, and Y. Shinohara, J. Therm. Anal. Calorim. **131**, 281 (2018).
[18] N. Haldolaarachchige, W. A. Phelan, Y. M. Xiong, R. Jin, J. Y. Chan, S. Stadler, and D. P. Young, J. Appl. Phys. **113**, 083709 (2013).

[19] Y. Takagiwa, Y. Matsubayashi, A. Suzumura, J. T. Okada, and K. Kimura, Mater. Trans. **51**, 988 (2010).
[20] W. G. Zeier, J. Schmitt, G. Hautier, U. Aydemir, Z. M. Gibbs, C. Felser, and G. J. Snyder, Nat. Rev. Mater. **1**, 16032 (2016).
[21] J. He, M. Amsler, Y. Xia, S. S. Naghavi, V. I. Hegde, S. Hao, S. Goedecker, V. Ozoliņš, and C. Wolverton, Phys. Rev. Lett. **117**, 046602 (2016).
[22] L. Huang, Q. Zhang, B. Yuan, X. Lai, X. Yan, and Z. Ren, Mater. Res. Bull. **76**, 107 (2016).
[23] F. Casper, T. Graf, S. Chadov, B. Balke, and C. Felser, Semicond. Sci. Technol. **27**, 063001 (2012).
[24] T. Yamada, V. L. Deringer, R. Dronskowski, and H. Yamane, Inorg. Chem. **51**, 4810 (2012).
[25] T. Yamada, T. Ikeda, R. P. Stoffel, V. L. Deringer, R. Dronskowski, and H. Yamane, Inorg. Chem. **53**, 5253 (2014).
[26] Y. F. Wang, Q. L. Xia, L. X. Pan, and Y. Yu, Trans. Nonferrous Met. Soc. China **24**, 1853 (2014).
[27] G. Kresse and J. Furthmüller, Comput. Mater. Sci. **6**, 15 (1996).
[28] G. Kresse and J. Furthmüller, Phys. Rev. B **54**, 11169 (1996).
[29] P. E. Blöchl, Phys. Rev. B **50**, 17953 (1994).
[30] G. Kresse and D. Joubert, Phys. Rev. B **59**, 1758 (1999).
[31] J. P. Perdew, K. Burke, and M. Ernzerhof, Phys. Rev. Lett. **77**, 3865 (1996).
[32] A. Togo and I. Tanaka, Scr. Mater. **108**, 1 (2015).
[33] A. Togo, L. Chaput, and I. Tanaka, Phys. Rev. B **91**, 094306 (2015).
[34] G. K. H. Madsen, J. Carrete, and M. J. Verstraete, Comput. Phys. Commun. **231**, 140 (2018).
[35] J. Heyd, G. E. Scuseria, and M. Ernzerhof, J. Chem. Phys. **124**, 219906 (2006).
[36] I. Terasaki, Y. Sasago, and K. Uchinokura, Phys. Rev. B **56**, R12685(R) (1997).
[37] B. B. Zhang, C. Wang, S. T. Dong, Y. Y. Lv, L. Y. Zhang, Y. D. Xu, Y. B. Chen, J. Zhou, S. H. Yao, and Y. F. Chen, Inorg. Chem. **57**, 2730 (2018).
[38] D. G. Cahill, S. K. Watson, and R. O. Pohl, Phys. Rev. B **46**, 6131 (1992).
[39] R. Guo, X. Wang, Y. Kuang, and B. Huang, Phys. Rev. B **92**, 115202 (2015).
[40] M. Christensen, A. B. Abrahamsen, N. B. Christensen, F. Juranyi, N. H. Andersen, K. Lefmann, J. Andreasson, C. R. H. Bahl, and B. B. Iversen, Nat. Mater. **7**, 811 (2008).
[41] D. J. Voneshen, K. Refson, E. Borissenko, M. Krisch, A. Bosak, A. Piovano, E. Cemal, M. Enderle, M. J. Gutmann, M. Hoesch, M. Roger, L. Gannon, A. T. Boothroyd, S. Uthayakumar, D. G. Porter, and J. P. Goff, Nat. Mater. **12**, 1028 (2013).
[42] P. C. Wei, S. Bhattacharya, J. He, S. Neeleshwar, R. Podila, Y. Y. Chen, and A. M. Rao, Nature (London) **539**, E1 (2016).
[43] P. K. Nair, M. T. S. Nair, and J. Campos, J. Electrochem. Soc. **140**, 539 (1993).
[44] O. Hellman and D. A. Broido, Phys. Rev. B **90**, 134309 (2014).
[45] A. Gaul, Q. Peng, D. J. Singh, G. Ramanath, and T. Borca-Tasciuc, Phys. Chem. Chem. Phys. **19**, 12784 (2017).
[46] X. Chen, D. Parker, and D. J. Singh, Phys. Rev. B **87**, 045317 (2013).
[47] Z. Tian, J. Garg, K. Esfarjani, T. Shiga, J. Shiomi, and G. Chen, Phys. Rev. B **85**, 184303 (2012).
[48] Y. L. Pei and Y. Liu, J. Alloys Compd. **514**, 40 (2012).
[49] E. Joseph and Y. Amouyal, J. Electron. Mater. **44**, 1460 (2014).
[50] Q. Tan, L. D. Zhao, J. F. Li, C. F. Wu, T. R. Wei, Z. B. Xing, and M. G. Kanatzidis, J. Mater. Chem. A **2**, 17302 (2014).
[51] N. Gothard, X. Ji, J. He, and T. M. Tritt, J. Appl. Phys. **103**, 054314 (2008).
[52] B. Peng, C. Yue, H. Zhang, Z. Fang, and H. M. Weng, npj Comput. Mater. **4**, 68 (2018).